



NUMERICAL STUDY OF MIXED CONVECTION HEAT TRANSFER ENHANCEMENT IN A HORIZONTAL CHANNEL BY ADDING METAL FOAM BLOCKS

Mohammed Abdulraouf Nim
Baghdad University- College of Engineering- Mechanical Engineering Department
dralsafi@uobaghdad.edu.iq

Abbas Husain Hajeej
Baghdad University- College of Engineering- Mechanical Engineering Department
abbas_eng1@yahoo.com

ABSTRACT :-

Mixed convection heat transfer in a horizontal channel supplied with metal foam blocks and partially heated at a constant heat flux is numerically investigated with air as the working fluid. The Brinkman-Forchheimer extended Darcy model is utilized to simulate the flow in the porous medium and the Navier-Stokes equation in the fluid region. The numerical investigations cover the Reynolds number range from 500 to 2000, heat fluxes varied from 500 to 6000 W/m², and Darcy number 5×10^{-2} to 1×10^{-3} . Results show that the wall temperatures at each heated section are affected by the imposed heat flux variation, Darcy and Reynolds numbers variation. The variations of the local heat transfer coefficient and the mean Nusselt number are presented and analysed. The mean Nusselt number enhancement was found to be more than 85% for all the studied cases from the fluid case.

KEYWORDS : convection heat transfer, metal foam, finite volume method, constant heat flux, horizontal channel.

دراسة عددية لتحسين انتقال الحرارة بالحمل المختلط في قناة أفقية بإضافة كتل من رغوة معدنية

محمد عبد الرؤوف نعمة عباس حسين هجيج

جامعة بغداد-كلية الهندسة- قسم الهندسة الميكانيكية

الخلاصة :-

أنتقال الحرارة بالحمل المختلط في قناة أفقية مزودة بكتل ذات رغوة معدنية ويتسخن جزئي بثبوت الفيض الحراري قد تم دراسته نظرياً مع استخدام الهواء كمائع مشغل. تم استخدام نموذج دارسي-برنكمان-فورشهيمر لمحاكاة الجريان في الوسط المسامي ومعادلة نقيير ستوك في منطقة المائع. شملت الدراسة النظرية لمدى رقم رينولدز من 500 الى 2000 وفيض حراري متغير من 500 واط/م² الى 6000 واط/م² ورقم دارسي 5×10^{-2} الى 1×10^{-3} . أظهرت النتائج تأثير درجات حرارة الجدار في كل جزء مسخن بتغير الفيض الحراري المسلط وتغير رقمي رينولدز ودارسي. تغير معامل أنتقال الحرارة الموضعي و متوسط رقم نسلت قد تم أظهارها وتحليلها. وجد أن التحسن في متوسط رقم نسلت أكثر من 85% لجميع الحالات التي تم دراستها في حالة المائع .

الكلمات المفتاحية: أنتقال الحرارة بالحمل، رغوه معدنية، طريقة الحجم المحكوم، فيض حراري ثابت، قناة أفقيه .

NOMENCLATURE :-

C = inertia coefficient.
 C_p = specific heat at constant pressure, J/kg.K.
 Da = Darcy number.
 F = Forchheimer coefficient.
 g = gravitational acceleration, m/s².
 Gr = Grashof number.
 H = channel height, m.
 h = local heat transfer coefficient, W/m².K.
 k = thermal conductivity of fluid, W/m.K.
 k_e = effective thermal conductivity, W/m.K.
 Nu = Nusselt number.
 p = pressure, pa.
 Pr = Prandtl Number.
 q = heat flux, W/m².
 Re = Reynolds number.
 Ri = Richardson number.
 R_μ = viscosity ratio.
 R_k = thermal conductivity ratio.
 K = permeability of the porous medium, m².
 s = porous block spacing, m.
 T = temperature, °C.
 u = axial velocity, m/s.
 v = transverse velocity, m/s.
 w = width of the copper foam block, m.

Greek Symbols

ν = kinematic viscosity, m²/s.
 β = thermal expansion coefficient, 1/K
 ε = porosity.
 μ = dynamic viscosity, kg m/s.
 ρ = density of air, kg/m³.

Subscripts

b = bulk.
 e = exit and effective.
 E = east
 g = global.
 m = mean.
 N = north
 S = south
 w = wall.
 W = west

INTRODUCTION :-

Convection heat transfer in a horizontal channel that supplied with heated metal foam blocks is a considerable technological interest. This is due to the wide range of applications such as electronic cooling, heat exchangers, nuclear power generation, filtration, and separation. A porous medium is considered as an effective enhancement method of heat transfer due to their intense mixing of the flow and their large surface area to volume ratio. Due to the random structures of porous mediums, they are different in their engineering, thermal and physical properties. Metal foams are a category of porous materials with unique properties that are utilized in heat transfer applications and several structural (Ashby et al., 2000). Metal foams are being produced as open-cell (functional) and closed-cell foams (structural). Open-cell metal foam consists of pores that are open to their neighboring pores and allow the fluid to pass through them. The closed-cell metal foams have a thin layer of metal dividing the individual pores. (Huang and Vafai, 1994) have performed a numerical study of forced convection in a channel with four porous blocks. The Brinkman-Forchheimer-extended Darcy model was utilized to simulate the flow in the porous medium and the Navier-Stokes equation in the fluid region. Results showed that an important heat transfer augmentation can be accomplished by adding the porous blocks. (Hadim, 1994) studied numerically the laminar forced convection in a fully or partially filled porous channel with discrete heated section flush-mounted on the bottom wall. Results showed that the Nusselt number increased when the Darcy number was decreased. Results also showed that the heat transfer in the both cases was almost the same increase (especially at low Darcy number), while the pressure drop was much lower in the partially filled channel. (Rachedi and Chick, 2001) numerically investigated the electronic cooling enhancement by supplement of foam materials. This method based on inserting the foam material between the elements on a horizontal board. The Darcy -Brinkman-Forchheimer model was utilized to describe the fluid motion in the foam materials. Results indicated that for a high thermal conductivity porous substrate, essential improvement was acquired compared to fluid case even if the permeability was less value. (Chikh et al., 1998) numerically studied force convection heat transfer in a horizontal channel, with evenly spaced porous blocks installed on the partially heated bottom wall. Results indicated that for the lower value of permeability, recirculation zones became clear between the blocks and prevented the fluid from passage through another block. The local Nusselt number was increased with a decreased in the wall temperature up to 90% by insertion of porous blocks. (Guerroudj and Kahalerras, 2010) studied numerically mixed convection in a horizontal channel supplied with porous blocks of different shapes that exposed to constant heat flux from the lower plate. The considered shapes vary from the triangular shape ($\gamma= 50.2^\circ$) to the rectangular shape ($\gamma= 90^\circ$). Results indicated that when the mixed convection (Gr/Re^2) increased, the global Nusselt number increased, especially at small values of permeability for triangular shape. At small values of the Reynolds number, Darcy number, thermal conductivity ratio and porous blocks height, the triangular shape lead to high rate of heat transfer. The highest pressure drop was found with the rectangular shape due to its volume, which the highest in comparison to the others shapes. (Kurtbas and Celik, 2009) experimentally investigated the mixed convective heat transfer in rectangular channel where the channel packed with open-cells aluminium foams with different number of pores per unit of length (PPI) with constant porosity ($\epsilon=0.93$). The channel was heated from the top and bottom by uniform heat flux. Results showed that the average Nusselt number increased relative to the pore densities. Results also showed that at high values of the Reynolds number and Grashof number, the local Nusselt number increased rapidly. (Chen et al., 2013) numerically studied forced convective cooling enhancement of a two-dimensional array of multiple heated sections mounted on the bottom wall of an insulated channel by using metal foam. Results indicated

that an increase in the fluid–solid interfacial heat exchange results in a decrease in the temperature difference between the fluid and solid phases for the same Reynolds number value, where the porous media tend to reach local thermal equilibrium (LTE) with the fluid and a higher cooling augmentation of heated sections was found. An experimental study was conducted by (Buonomo et al., 2014) for mixed convection in the air in a heated channel partially filled with aluminium foam. The aluminium foam layer was put on the bottom plate of the channel heated. Results also showed that the influence of the aluminium foams appears more significant for the high Reynolds number values and mean Nusselt number increases with the existence of the aluminium foam in the channel. In the present work, mixed convection heat transfer in a horizontal channel that supplied with metal foam (copper foam) blocks and exposed to a constant heat flux, is numerically examined with air as the working fluid. The main objective is to study the effect of convection heat transfer on the flow field and the associated heat transfer process in such system. The influence of heat flux, Darcy number, and Reynolds number variation on isotherms, streamlines, velocity vector and the heat transfer rate at the heated section in terms of local heat transfer coefficient and mean Nusselt number are investigated and analysed .

MATHEMATICAL FORMULATION

Geometry and Coordinate System

The geometry and coordinate system for mixed convection heat transfer in a channel that supplied with metal foam blocks and exposed to a constant heat flux as shown in **Fig.1**. The system under investigation is a two-dimensional horizontal channel. The top wall is thermally insulated while metal foam blocks of width (w), spacing (s), height (H), and heated from lower are attached to the bottom wall at three different locations. The remaining of the channel is adiabatic as shown in **Fig.1**. The air enters the channel with a constant temperature and a uniform velocity. The length behind the last block is selected high enough so that a fully developed condition at the exit can be assumed .

Assumptions

To solve the flow and heat transfer equations (conservation of mass, momentum and energy) some assumptions should be made to simplify the problem:

- 1) Laminar flow.
- 2) Steady state.
- 3) Boussinesq approximation is used, which consists of the following:
 - a. Density is assumed constant except when it directly causes buoyant forces (in momentum equation).
 - b. All other fluid properties are assumed constant.
- 4) Incompressible fluid.
- 5) Two- dimensional air flow.
- 6) No internal heat generation and neglecting viscous dissipation.
- 7) Homogeneous, isotropic porous medium.
- 8) The solid matrix of the porous medium is considered in a local thermal equilibrium with the passing fluid .

Governing Equations

According to the above assumptions, the basic equations are reduced to the following equations (1) to (6), mass, momentum and energy equation for the flow between parallel plate channels. In the present study the Brinkman- Forchheimer extended Darcy model (Vafai and Tien, 1981) is used to model the flow in the porous regions, the Navier-Stokes equations in the fluid regions, and the thermal field is considered by the energy equation as follows;

Conservation of mass

$$\frac{\partial u}{\partial x} + \frac{\partial v}{\partial y} = 0 \quad (1)$$

Conservation of momentum

without metal foam (fluid case)

x-Momentum Equation:

$$\rho \left(u \frac{\partial u}{\partial x} + v \frac{\partial u}{\partial y} \right) = -\frac{\partial P}{\partial x} + \mu \left(\frac{\partial^2 u}{\partial x^2} + \frac{\partial^2 u}{\partial y^2} \right) \quad (2)$$

y-Momentum Equation:

$$\rho \left(u \frac{\partial v}{\partial x} + v \frac{\partial v}{\partial y} \right) = -\frac{\partial P}{\partial y} + \mu \left(\frac{\partial^2 v}{\partial x^2} + \frac{\partial^2 v}{\partial y^2} \right) + \rho g \beta (T - T_{in}) \quad (3)$$

with metal foam

x-Momentum Equation:

$$\frac{\rho}{\varepsilon^2} \left(u \frac{\partial u}{\partial x} + v \frac{\partial u}{\partial y} \right) = -\frac{\partial p}{\partial x} + \mu_e \left(\frac{\partial^2 u}{\partial x^2} + \frac{\partial^2 u}{\partial y^2} \right) - \frac{\mu}{K} u - \frac{\rho F \varepsilon}{\sqrt{K}} |\vec{V}| u \quad (4)$$

y-Momentum Equation:

$$\frac{\rho}{\varepsilon^2} \left(u \frac{\partial v}{\partial x} + v \frac{\partial v}{\partial y} \right) = -\frac{\partial p}{\partial y} + \mu_e \left(\frac{\partial^2 v}{\partial x^2} + \frac{\partial^2 v}{\partial y^2} \right) - \frac{\mu}{K} v - \frac{\rho F \varepsilon}{\sqrt{K}} |\vec{V}| v + \rho g \beta (T - T_{in}) \quad (5)$$

Conservation of energy

$$\rho C_p \left(u \frac{\partial T}{\partial x} + v \frac{\partial T}{\partial y} \right) = k_e \left(\frac{\partial^2 T}{\partial x^2} + \frac{\partial^2 T}{\partial y^2} \right) \quad (6)$$

where $|\vec{V}| = \sqrt{u^2 + v^2}$. The porosity (ε), the metal foam permeability (K), thermal conductivity and the effective viscosity are taken respectively to unity ($\varepsilon = 1$), infinity ($K \rightarrow \infty$) and thermal conductivity and fluid's viscosity in the fluid region. The term $-\frac{\mu}{K} \vec{V} - \frac{\rho F \varepsilon}{\sqrt{K}} |\vec{V}| \vec{V}$ can be noticed as the resistance offered by the metal foam to the flow.

Boundary Conditions

At the inlet: $x = 0; 0 < y < H: u = u_{in}; v = 0$ and $T = T_{in}$

At the exit: $x = l; 0 < y < H: \frac{\partial u}{\partial x} = 0; v = 0$ and $\frac{\partial T}{\partial x} = 0$

At the lower plate: $y = 0; 0 < x < l: u = v = 0$ and $\frac{\partial T}{\partial y} = \begin{cases} -\frac{q}{k_e} & \text{under the porous blocks} \\ 0 & \text{elsewhere} \end{cases}$

At the upper plate: $y = H; 0 < x < l: u = v = 0$ and $\frac{\partial T}{\partial y} = 0$

Nondimensionalization

To nondimensionalize the variables used in the governing equations, the following dimensionless variables are defined (**Guerroudj and Kahalerras, 2010**);

$$X = \frac{x}{H}; Y = \frac{y}{H}; U = \frac{u}{u_{in}}; V = \frac{v}{u_{in}}; P = \frac{p}{\rho u_{in}^2} \text{ and } \theta = \frac{T - T_{in}}{q \frac{H}{k}}$$

$$Re = \frac{u_{in}H}{\nu}; Ri = \frac{Gr}{Re^2}; Da = \frac{K}{H^2}; Gr = \frac{g\beta \frac{qH}{k} H^3}{\nu^2}; Pr = \frac{\mu C_p}{k}; C = \varepsilon F; R_\mu =$$

$$\frac{\mu_e}{\mu} \text{ and } R_k = \frac{k_e}{k}$$

These parameters are substituted into equations (1) to (6), the resulting equations are as follows;

$$\frac{\partial U}{\partial X} + \frac{\partial V}{\partial Y} = 0 \quad (7)$$

$$\frac{1}{\varepsilon^2} \left(U \frac{\partial U}{\partial X} + V \frac{\partial U}{\partial Y} \right) = -\frac{\partial P}{\partial X} + \frac{R_\mu}{Re} \left(\frac{\partial^2 U}{\partial X^2} + \frac{\partial^2 U}{\partial Y^2} \right) - \frac{1}{Re Da} U - \frac{C}{\sqrt{Da}} |\vec{V}| U \quad (8)$$

$$\frac{1}{\varepsilon^2} \left(U \frac{\partial V}{\partial X} + V \frac{\partial V}{\partial Y} \right) = -\frac{\partial P}{\partial Y} + \frac{R_\mu}{Re} \left(\frac{\partial^2 V}{\partial X^2} + \frac{\partial^2 V}{\partial Y^2} \right) - \frac{1}{Re Da} V - \frac{C}{\sqrt{Da}} |\vec{V}| V + \frac{Gr}{Re^2} \theta \quad (9)$$

$$U \frac{\partial \theta}{\partial X} + V \frac{\partial \theta}{\partial Y} = \frac{R_k}{Re Pr} \left(\frac{\partial^2 \theta}{\partial X^2} + \frac{\partial^2 \theta}{\partial Y^2} \right) \quad (10)$$

The boundary conditions in dimensionless form can be written as:

At the inlet: $X = 0; 0 < Y < 1; U = 1; V = 0$ and $\theta = 0$

At the exit: $X = L; 0 < Y < 1; \frac{\partial U}{\partial X} = 0; V = 0$ and $\frac{\partial \theta}{\partial X} = 0$

At the lower plate: $Y = 0; 0 < X < L; U = V = 0$ and $\frac{\partial \theta}{\partial Y} = \begin{cases} -\frac{1}{R_k} & \text{under the porous blocks} \\ 0 & \text{elsewhere} \end{cases}$

At the upper plate: $Y = 1; 0 < X < L; U = V = 0$ and $\frac{\partial \theta}{\partial Y} = 0$

At interfacial conditions (**Fu et al., 1996**) on surface **AB** and **CD** (see **Fig. 1**):

$$U|_f = U|_{por.}, V|_f = V|_{por.}, P|_f = P|_{por.}, \frac{\partial U_f}{\partial X} = \frac{\partial U_{por.}}{\partial X}, \frac{\partial V_f}{\partial X} = \frac{\partial V_{por.}}{\partial X}$$

$$\theta_f = \theta_{por.}, k_f \frac{\partial \theta_f}{\partial X} = k_e \frac{\partial \theta_{por.}}{\partial X}$$

FURTHER CALCULATIONS

The Nusselt Number

The local heat transfer coefficient at the heated wall can be defined as:

$$h = \frac{q}{T_w - T_b} \quad (11)$$

Hence, the local and the mean Nusselt number can be defined as, (**Nield and Bejan, 2006**):

$$Nu = \frac{hH}{k} = \frac{qH/k}{(T_w - T_b)} = \frac{1}{\theta_w - \theta_b} \quad (12)$$

$$Nu_m = \frac{1}{W} \int_{X_1}^{X_1+W} Nu dX \quad (13)$$

where X_i is the location of the block i from the channel inlet, θ_w is the dimensionless wall temperature, and θ_b is the dimensionless bulk temperature can be defined as:

$$\theta_b = \frac{\int_0^1 |u| \theta dY}{\int_0^1 |u| dY} \quad (14)$$

The global Nusselt number can be written as:

$$Nu_g = \frac{\sum_{i=1}^N Nu_{mi}}{N} \quad (15)$$

where N is the number of blocks attached in the channel.

Effective Thermal Conductivity

An important property of the porous medium is the effective thermal conductivity (k_e). To estimate the effective thermal conductivity of open-cell metal foam, k_e , the following correlation was proposed by (Calmidi and Mahajan, 1999) as;

$$k_e = \varepsilon k_{air} + 0.181(1 - \varepsilon)^{0.763} k_s \quad (16)$$

where the air thermal conductivity k_{air} is taken as 0.0263 W/m.K and Thermal conductivity of the copper foams k_s (386 W/m.K) (Holman, 2010).

NUMERICAL PROCEDURE :-

Numerical methods represent a useful alternative to analytical solution. Such methods have proven to be increasingly popular. In the present work, the velocity and pressure fields in equations (8) and (9) are linked by the SIMPLE algorithm of (Patanker, 1980). The obtained system of algebraic equations is then solved by the finite volume method with a line-by-line tri-diagonal matrix algorithm TDMA. The energy equation (10) was solved by a fully implicit control volume-based finite difference formulation with the use of the power law scheme of (Patanker, 1980), to discretize the combined convective and conductive terms. A computer program was build using MATLAB R2013a to implement the above procedure and to solve the governing equations. The flow chart of the built computer program is shown in Fig. 2.

Before proceeding further, the grid independency tests are performed first. Numerical tests were performed for various grid sizes 357 x 151, 391 x 151 and 447 x 121 to test and estimate the grid independent solutions. It is observed that the global Nusselt number value does not exceed 3% see Table 1. Therefore, a grid size of 391x 151 is chosen for further computation because it consumed less computing time. A non-uniform grid system is used in the X direction to provide a fine grid generation in the test section that supplied with metal foam blocks [inlet section (45), test section (166), and exit section (180)] as shown in Fig. 3. A relative error less than 10^{-5} is required for both the velocity and temperature fields between successive iterations (for the global Nusselt number), and the normalized residual for the pressure field are less than 10^{-7} to achieve convergence.

$$\bar{R} = \frac{\sum |a_E \phi_E + a_W \phi_W + a_N \phi_N + a_S \phi_S + b - a_P \phi_P|}{\sum |a_P \phi_P|} \leq 10^{-7} \quad (17)$$

CODE VALIDATION

To validate the present code, a comparison was made with (**Guerroudj and Kahalerras, 2010**) results. The channel was provided with metal foam blocks of porosity ($\varepsilon=0.97$), inertial coefficient ($C=0.1$) and subjected to constant heat fluxes from lower wall and the other side is adiabatic. **Fig. 4** shows a good matching with (**Guerroudj and Kahalerras, 2010**) result.

RESULTS AND DISCUSSION

In the present study, the problem of mixed convection heat transfer through a horizontal channel supplied with metal foam blocks that subjected to constant heat flux at each heated section is solved based on the thermal equilibrium model. Numerical computations were performed for a horizontal channel of 0.1 m height, 1.9 m length [inlet section ($l_i=0.15\text{m}$), test section (0.25m), and exit section ($l_e=1.5\text{m}$)], $w=0.05$ m (width of metal foam block), and $s=0.05$ m (space between block) as shown in **Fig.1**. The channel is provided with three metal foam blocks (copper). The properties of the metal foam and air that used in the present study are listed in **Table 2**.

Streamlines, Velocity Vectors, and Temperature Contours

Fig.5 shows the effect of insert metal foam blocks on the streamlines at each heated section for $q=500\text{ W/m}^2$ and $Re=1000$. It can be seen that the distortion of the streamlines in the case of insert metal foam blocks become more pronounced from the case of without metal foam blocks (fluid case) due to the presence of metal foam block array.

Fig.6 shows the influence of insert metal foam blocks on the velocity distribution at each heated section for $q=500\text{ W/m}^2$ and $Re=1000$. It can be seen that the velocity near the heated sections in the case of insert metal foam blocks become larger from that in the case of without metal block (fluid case). This can be attributed to the fact that the bulk damping and viscous influences are restricted to the zone near at each heated section.

Fig.7 shows the effect of insert metal foam blocks on the temperature contours along a horizontal channel for $q=500\text{ W/m}^2$, $Re=1000$. It can be seen that the temperature contours in the case of insert metal foam blocks is much lower than that in the case of without metal foam blocks (fluid case). The presence of the metal foam blocks enhanced the overall heat transfer; part of heat is transferred from the heated section by mean of conduction through the metal foam blocks and the other part by mean of convection to the incoming fluid that passed over the heated section.

Fig.8 shows the influence of the imposed heat flux variation on the temperature contours along a horizontal channel for $Re=600$, and $Da=1 \times 10^{-3}$. It can be seen that temperature is increased at each heated section as the heat flux increased for the same Reynolds number value. When the imposed heat flux is increased, the buoyancy effect increases and causes a faster growth in the thermal boundary layer along the surface at each heated section.

Fig.9 shows the effect of Reynolds number variation on the temperature contours along a horizontal channel for $q = 1000\text{ W/m}^2$, and $Da=1 \times 10^{-3}$. It is obvious that the increasing of Reynolds number reduces the wall temperature at each heated section for the same heat flux value. When the Reynolds number is increased the thermal boundary layer retreat along the heated wall at each heated section .

Wall Temperature Distribution of the Heated Section

Fig.10 shows the effect of insert metal foam blocks on the wall temperature distribution at each heated section for $q=500 \text{ W/m}^2$, $Re=1000$, and $Da=5 \times 10^{-2}$, 1×10^{-2} , 1×10^{-3} , respectively. It can be seen that the wall temperature in the case of insert metal foam blocks is much lower than that in the case of without metal foam blocks (fluid case). The presence of the metal foam blocks caused part of heat to transfer from the heated section by mean of conduction through the metal foam blocks and the other part by mean of convection to the incoming fluid that passed over the heated section. The conducted heat through the metal foam block is then transferred to the incoming fluid by means of convection due to the high mixing that provided by the metal foam. The above mechanism that works in the case of metal foam presence increased the heat transfer from the heated section to the incoming fluid and increases the bulk temperature of air which means that air will gain more heat from the hot wall which leads to decrease the wall temperature at each heated section. The wall temperature at each heated section reduces more with a Darcy number decrease because of increasing in mixing which leads to increase in convected heat by air.

Local Heat Transfer Coefficient

A general behavior can be seen from the distribution of the local heat transfer coefficient in **Figs. 11** and **12** that the local heat transfer coefficient in all cases decreases with increase in the axial distance at each heated section. Since the heat transfer coefficient is based on the temperature difference with respect to the bulk temperature, this trend is expected as the largest temperature difference between the heated wall and the incoming cold fluid occurs at the leading edge of the heated section especially at higher Reynolds number. Therefore, the highest heat transfer rate occurs at the leading edge of the heated section especially at first heated section which is nearest to the inlet

Fig.11 shows the influence of Reynolds number variation on the distribution of the local heat transfer coefficient at each heated section for $q = 3000 \text{ W/m}^2$ and $Da= 1 \times 10^{-3}$. It can be seen that the local heat transfer coefficient is increased as the Reynolds number increased for the same heat flux value. When the Reynolds number is increased, a reduction in the thermal boundary layer thickness occurs with the domination of the incoming cold-fluid effect and this will cause a larger fluid mixing and higher local heat transfer coefficient values especially at first heated section which is nearest to the inlet.

Fig.12 shows the influence of the imposed heat flux variation on the distribution of the local heat transfer coefficient at each heated section for $Re =600$ and $Da=1 \times 10^{-3}$. It can be seen that the local heat transfer coefficient is increased at each heated section as the heat flux increased for the same Reynolds number value. This can be attributed to the fact that for higher heat fluxes the buoyancy effect increases and the thermal boundary layer growth is more rapidly and causes a smaller temperature difference between the fluid bulk temperature and the heated wall temperature at each heated section.

Fig.13 shows the effect of Darcy number on the local heat transfer coefficient at each heated section for $q= 500 \text{ W/m}^2$ and $Re=1000$. It can be seen that the local heat transfer coefficient in the case of insert metal foam blocks is much higher than that in the case of without metal foam blocks (fluid case). **Fig.13** also shows that the local heat transfer coefficient for lower Darcy Number ($Da=1 \times 10^{-3}$) is higher than that for higher Darcy Number ($Da= 5 \times 10^{-2}$ and $Da= 1 \times 10^{-2}$). This can be attributed to the heat transfer enhancement that caused by the higher fluid mixing in the lower Darcy number metal foam block .

Mean Nusselt Number

A general behavior can be seen from **Figs.14-16** that the maximum mean Nusselt number value is located at the first block. This trend is expected as the largest temperature difference between the heated wall and the incoming cold fluid occurs at the first block. Therefore, the highest heat transfer rate occurs at the first heated section.

Fig.14 shows the influence of Reynolds number variation on the mean Nusselt Number at each block for $q = 2000 \text{ W/m}^2$ and $Da = 1 \times 10^{-3}$. It can be seen that the mean Nusselt number is increased at each block as the Reynolds number increased for the same heat flux value. This can be attributed to the higher fluid mixing that associated with the domination of the incoming cold-fluid effect.

The variation of the mean Nusselt number with imposed heat flux along the heated wall at each block is presented in **Fig.15** for $Re=500$ and $Da = 1 \times 10^{-3}$. It can be noticed from **Fig.15** that the mean Nusselt number is increased as the heat flux increased at each block number for the same Reynolds number value.

Fig.16 shows the effect of Darcy number on the mean Nusselt number at each block for $q = 500 \text{ W/m}^2$ and $Re=1000$. It can be seen that the mean Nusselt number in case insert of metal foam blocks enhanced the heat transfer from the heated sections compared with the pure fluid case. **Fig.16** also indicate that the mean Nusselt number for $Da = 1 \times 10^{-3}$ is higher than that of $Da = 5 \times 10^{-2}$ and $Da = 1 \times 10^{-2}$ due to the higher fluid mixing in the lower Darcy number. The adding of the metal foam blocks caused a remarkable enhancement in the mean Nusselt number from that in the fluid case as in case of $q=500 \text{ W/m}^2$ and $Re=1000$ (98%) for $Da = 1 \times 10^{-3}$, $Da = 1 \times 10^{-2}$, and $Da = 5 \times 10^{-2}$.

Correlations of the Global Nusselt Number

The values of the global Nusselt number Nu_g for the present experimental work are plotted in **Fig. (17)** in the form of Nu_g against Ri for the range of $11 \leq Ri \leq 500$. The correlation equations are calculated for each case of metal foam.

- For $Da = 1 \times 10^{-2}$

$$Nu_g = 1420.8 (Ri)^{-0.015} \quad (18)$$

- For $Da = 1 \times 10^{-3}$

$$Nu_g = 1527.5 (Ri)^{-0.023} \quad (19)$$

CONCLUSIONS

The main conclusions of the present work are:

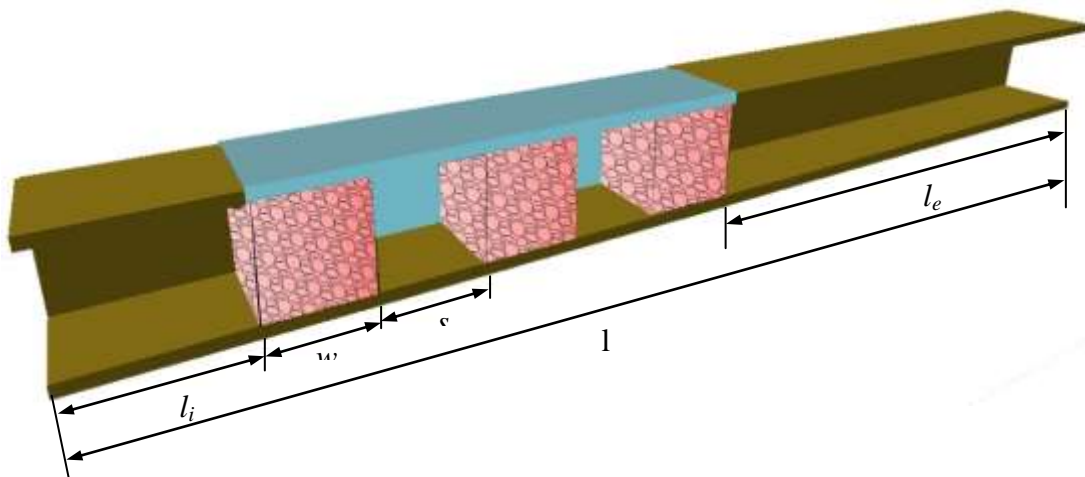
- 1- The wall temperature at each heated section increases as the imposed heat flux is increased for the two cases, without (fluid case) and with metal foam blocks.
- 2- The local heat transfer coefficient and the mean Nusselt number is increased with the decreased of the Darcy number.
- 3- The enhancement in the mean Nusselt number for all the studied cases is over 85 % from the fluid case.

Table 1. Grid Sensitivity Analysis

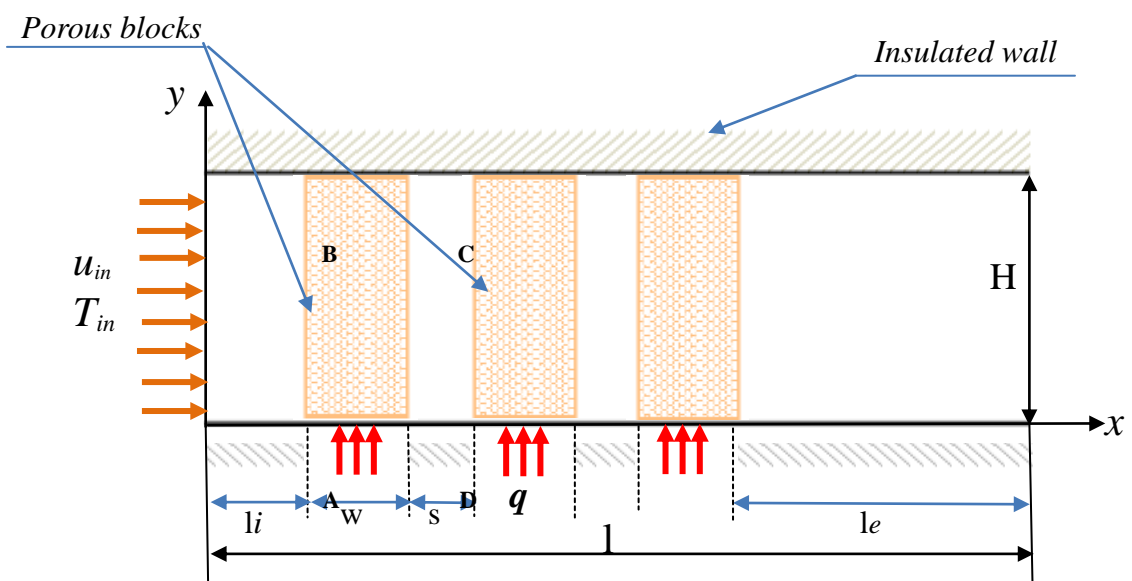
| m x n | Nu_g | Relative difference (%) |
|-----------|--------|-------------------------|
| 357 x 151 | 885.92 | — |
| 391 x 151 | 886.1 | 0.02 |
| 447 x 121 | 908.88 | 2.5 |

Table 2. Properties of Metal Foam and Air

| | | | | | |
|-------------|------------|-----------|--------|---------------|---------------|
| Copper foam | ϵ | C | R_k | R_μ | k_s (W/m.K) |
| | 0.903 | 0.17 | 449.86 | 1 | 386 |
| Air | Pr | k (W/m.K) | | T_{in} (°C) | |
| | 0.7 | 0.0263 | | 40 | |



(a) 3-D Project



(b) 2-D Project

Figure 1 . Schematic of the physical domain.

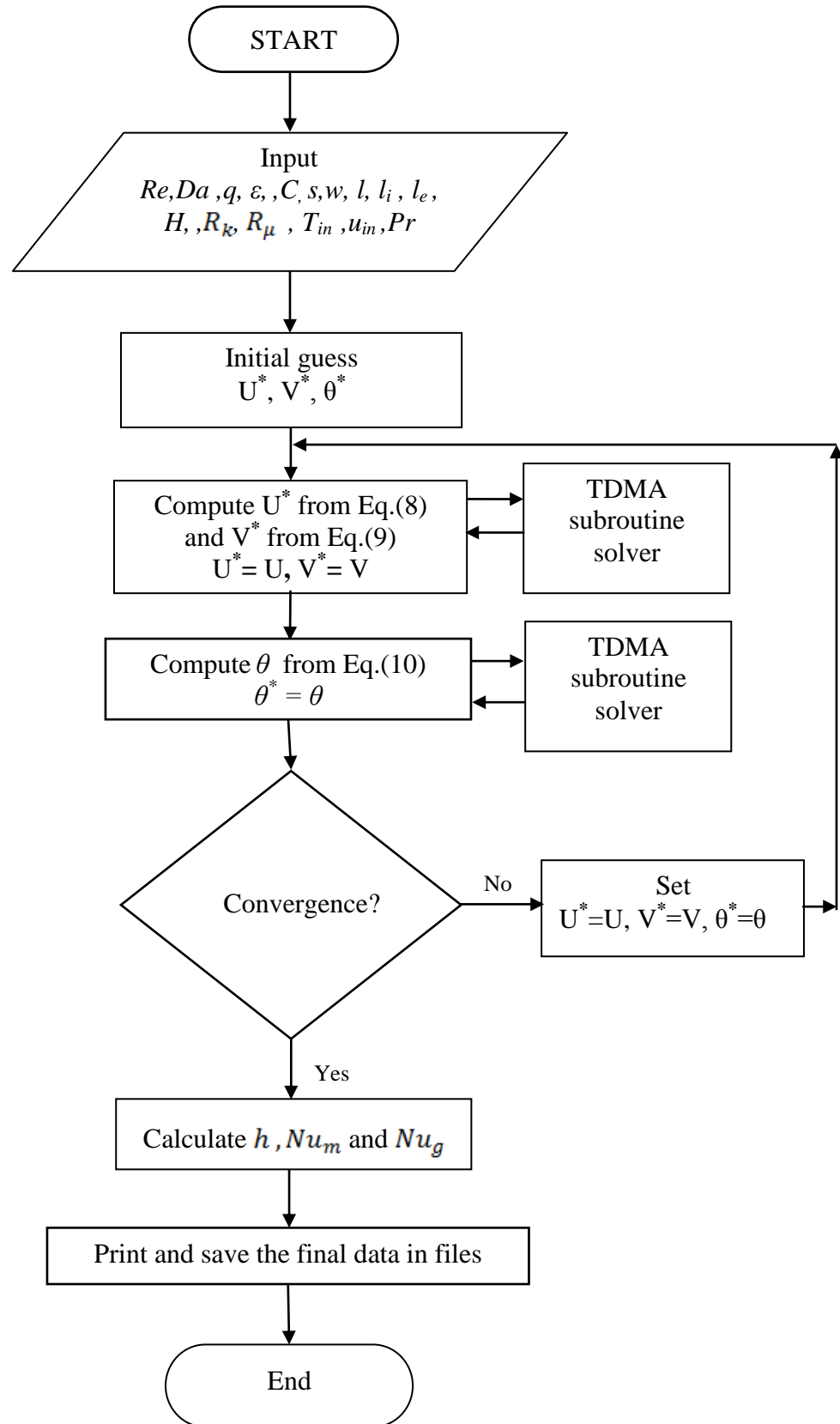


Figure 2. Flow Chart for the Computer Program.

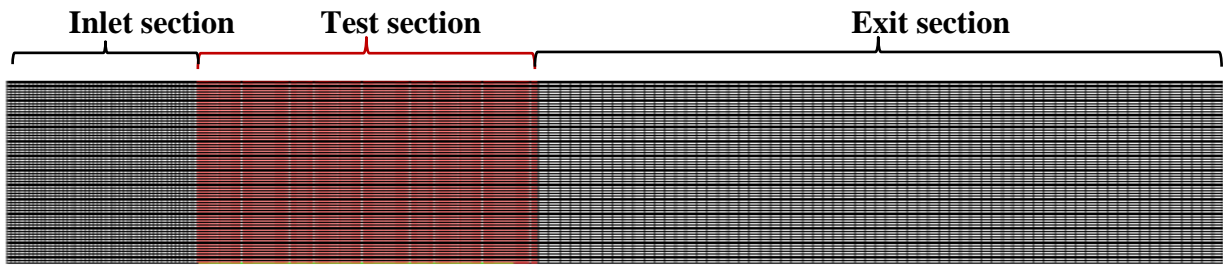


Figure 3. Non uniform grid generation.

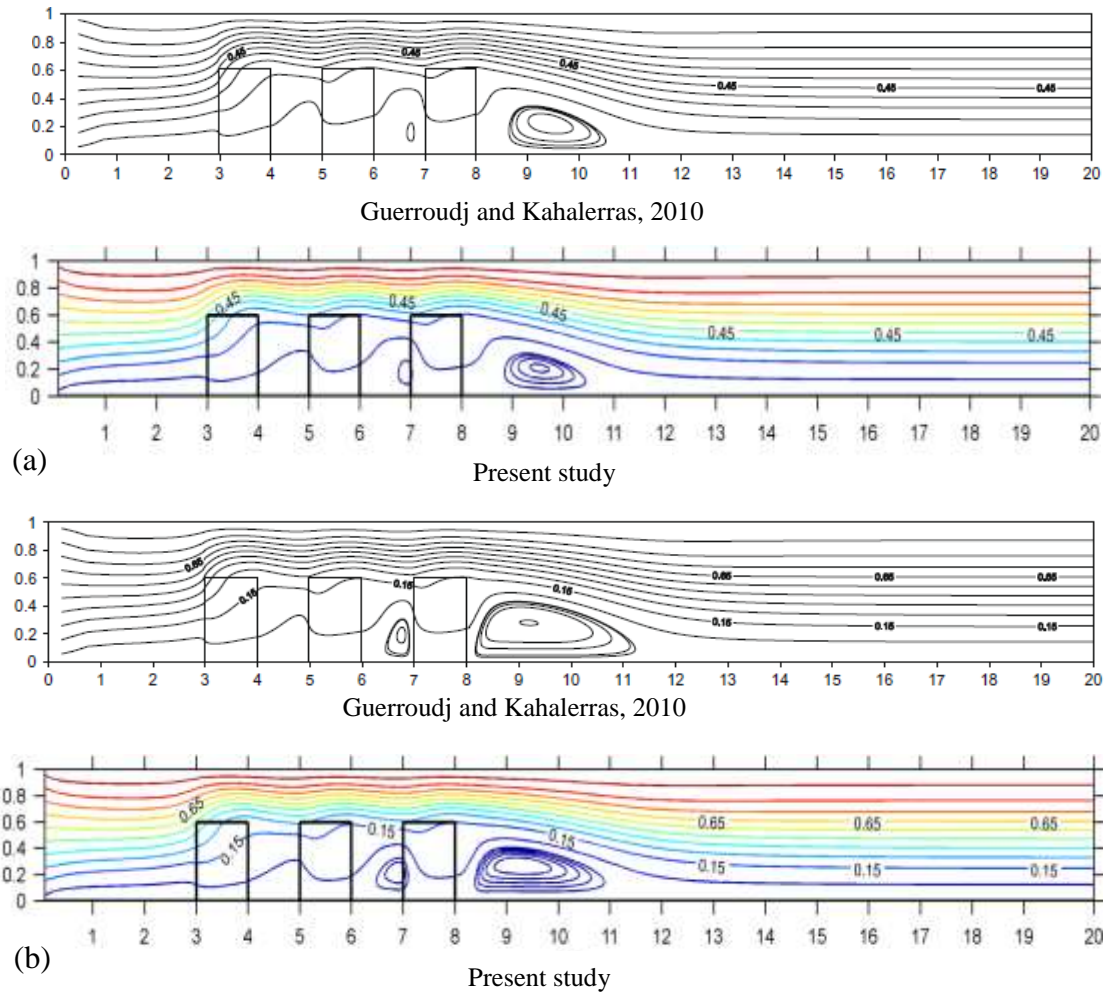


Figure 4. Streamlines for $Re=100$, $H_p=0.6$, $R_k=1$ and $Da=1 \times 10^{-3}$
 (a) $Ri=0$ (b) $Ri=20$.

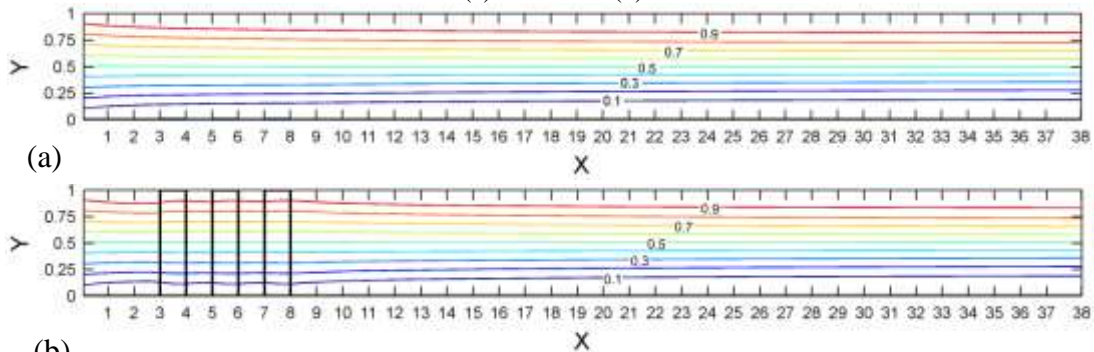


Figure 5. Streamlines for $Re=1000$ and $q=500 \text{ W/m}^2$
 (a) Fluid case (b) With metal foam ($Da=1 \times 10^{-3}$).

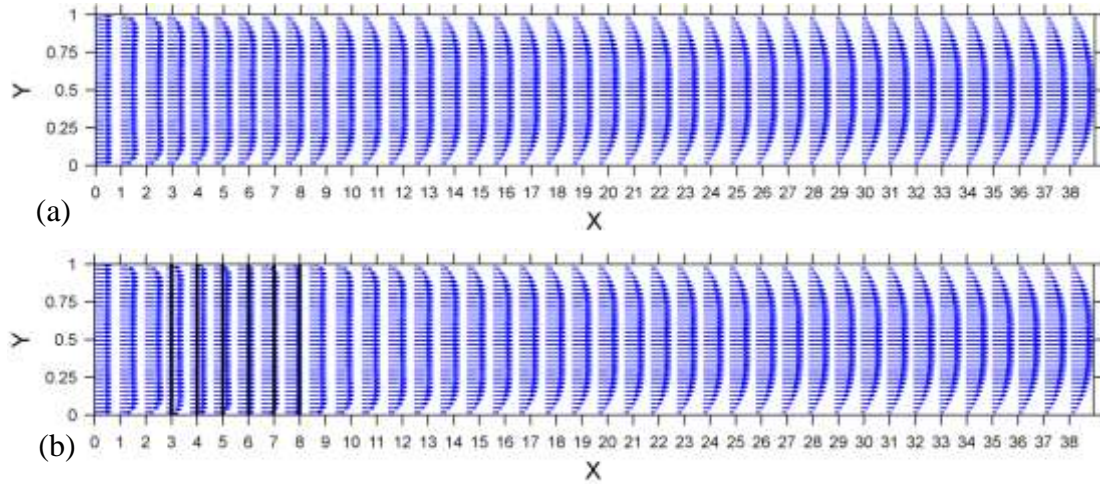


Figure 6. Velocity vectors for $Re=1000$ and $q=500 \text{ W/m}^2$
(a) Fluid case (b) With metal foam ($Da=1 \times 10^{-3}$).

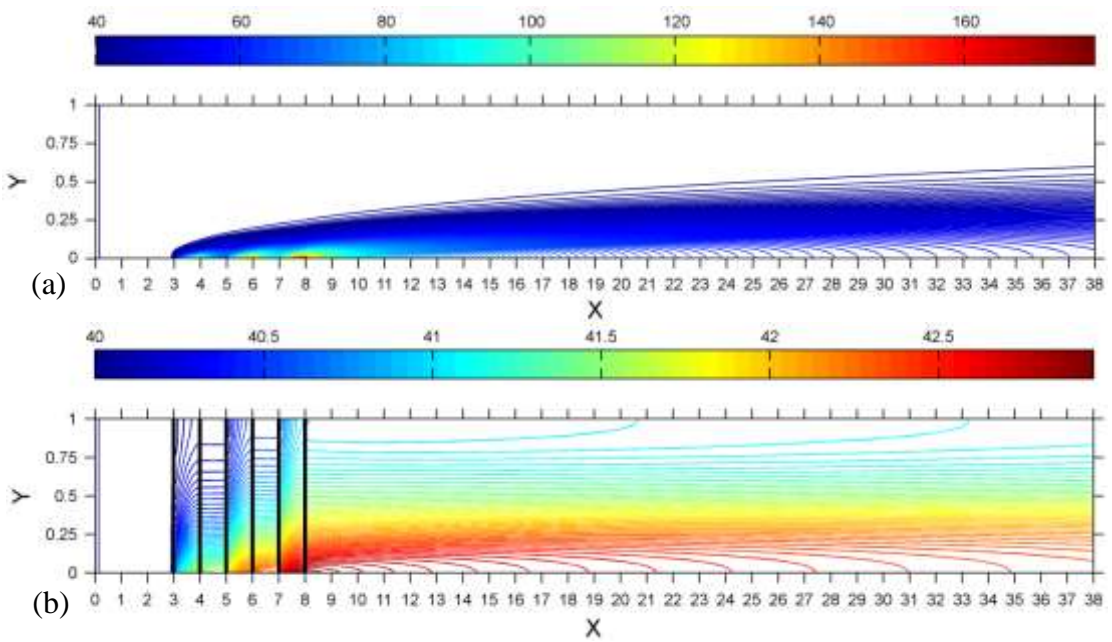


Figure 7. Temperature contours ($^{\circ}\text{C}$) for $Re=1000$ and $q=500 \text{ W/m}^2$
(a) Fluid case (b) With metal foam ($Da=1 \times 10^{-3}$)

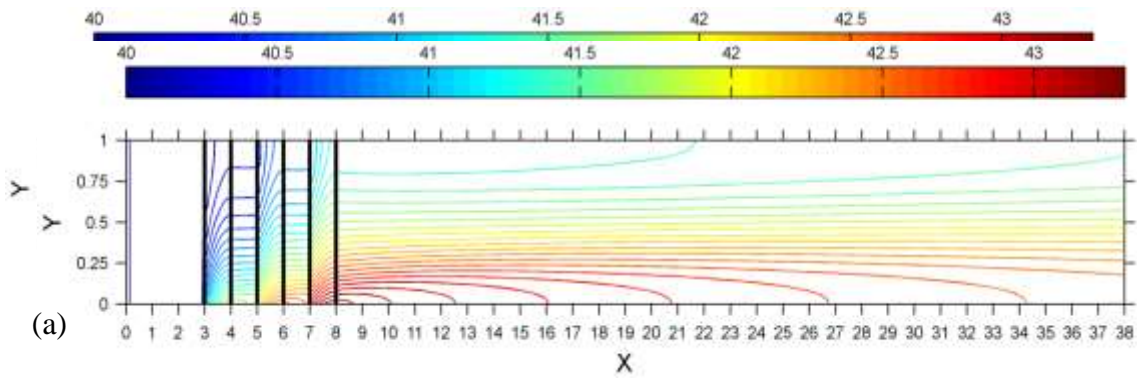


Figure 8. Temperature contours (°C) for $Re=600$ and $Da=1 \times 10^{-3}$
(a) $q=500 \text{ W/m}^2$ (b) $q=1500 \text{ W/m}^2$ (c) $q=2000 \text{ W/m}^2$

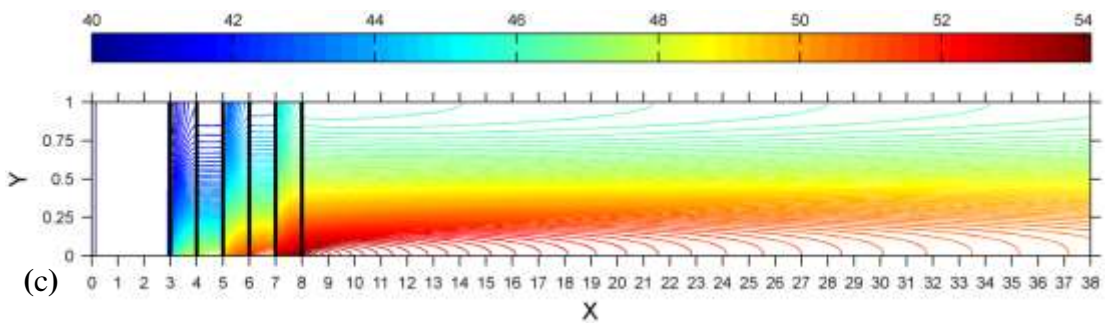
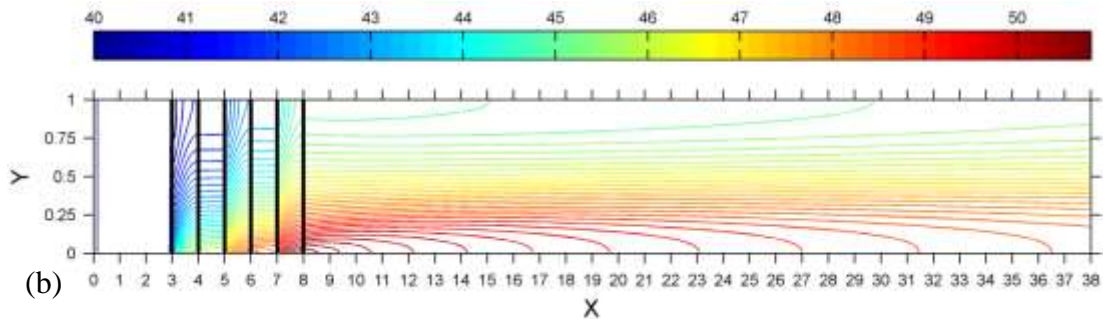


Figure 8. Continued

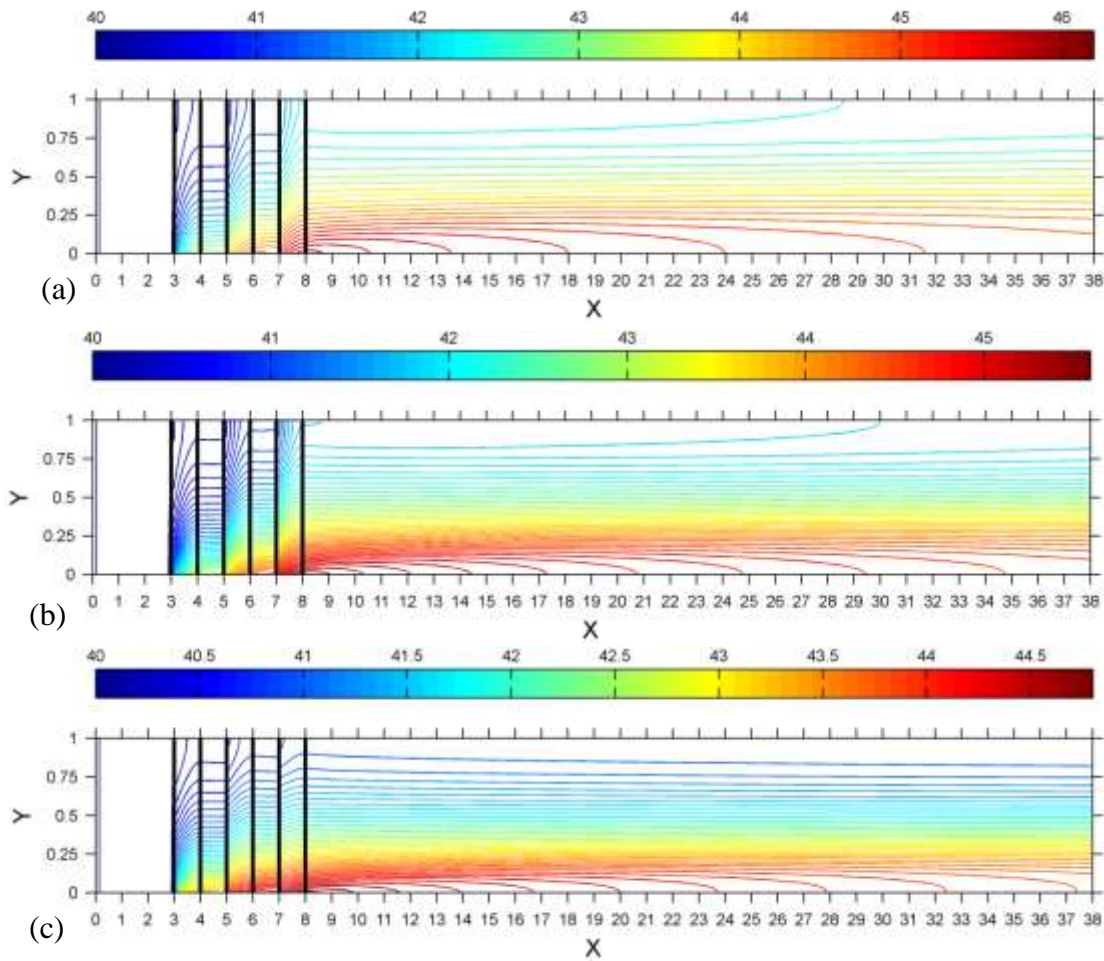


Figure 9 . Temperature contours (°C) for $q=1000 \text{ W/m}^2$ and $Da=1 \times 10^{-3}$
(a) $Re=800$ (b) $Re=1300$ (c) $Re=2000$.

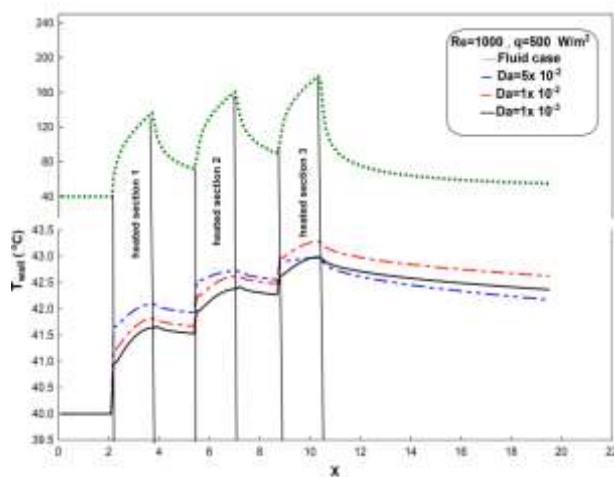


Figure 10. Variation of the wall Temperature with the axial distance for different Darcy number.

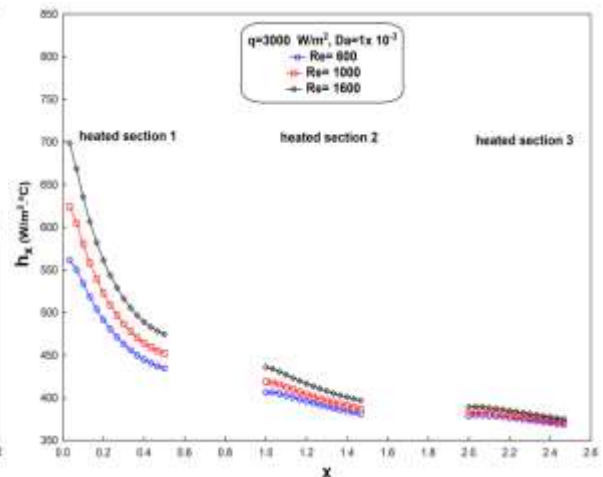


Figure 11. Local heat transfer coefficient with the axial distance for different Reynolds number.

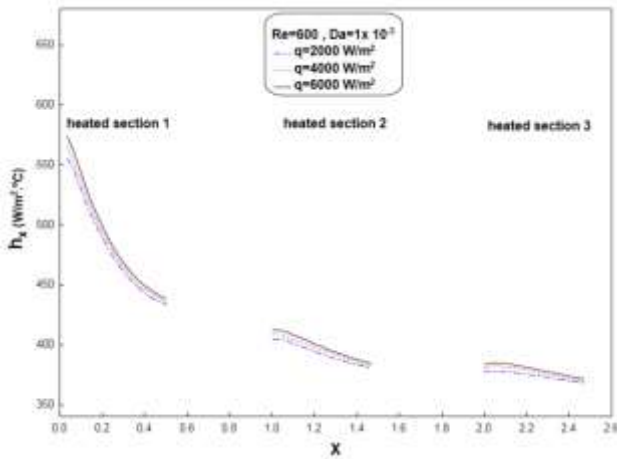


Figure 12. Local heat transfer coefficient with the axial distance for different heat

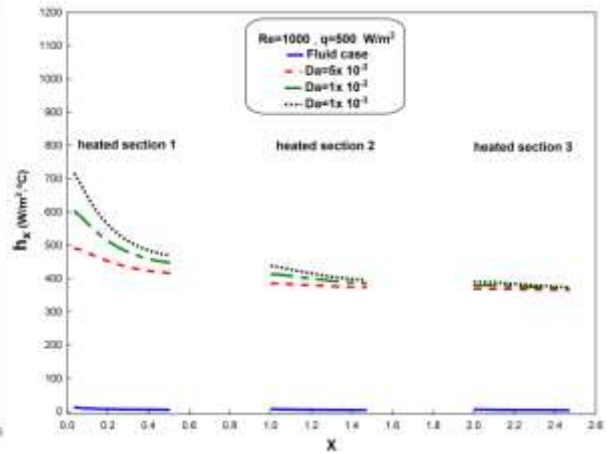


Figure 13. Local heat transfer coefficient with the axial distance for different Darcy

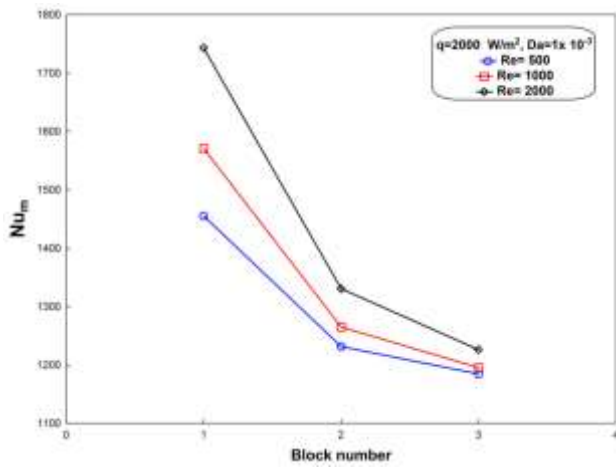


Figure 14. Mean Nusselt number with block number for different Reynolds number.

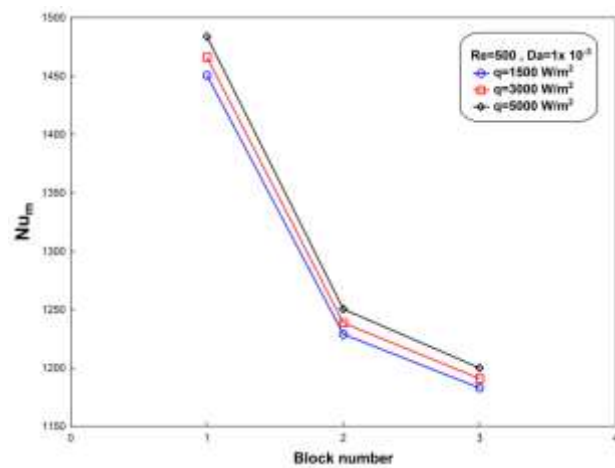


Figure 15. Mean Nusselt number with block number for different heat fluxes.

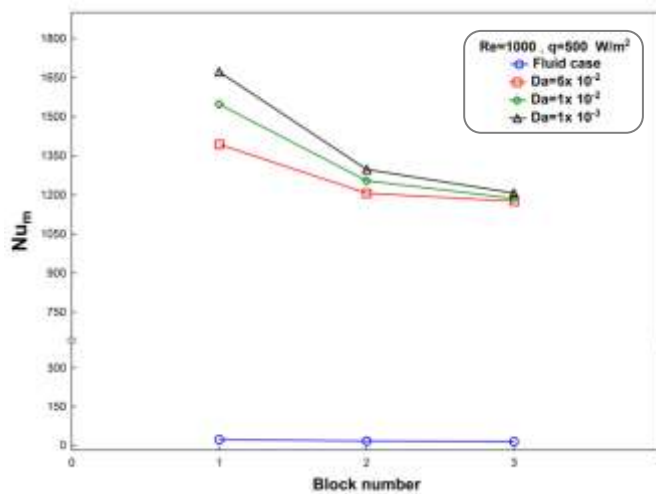


Figure 16. Mean Nusselt number with block number: different Darcy number.

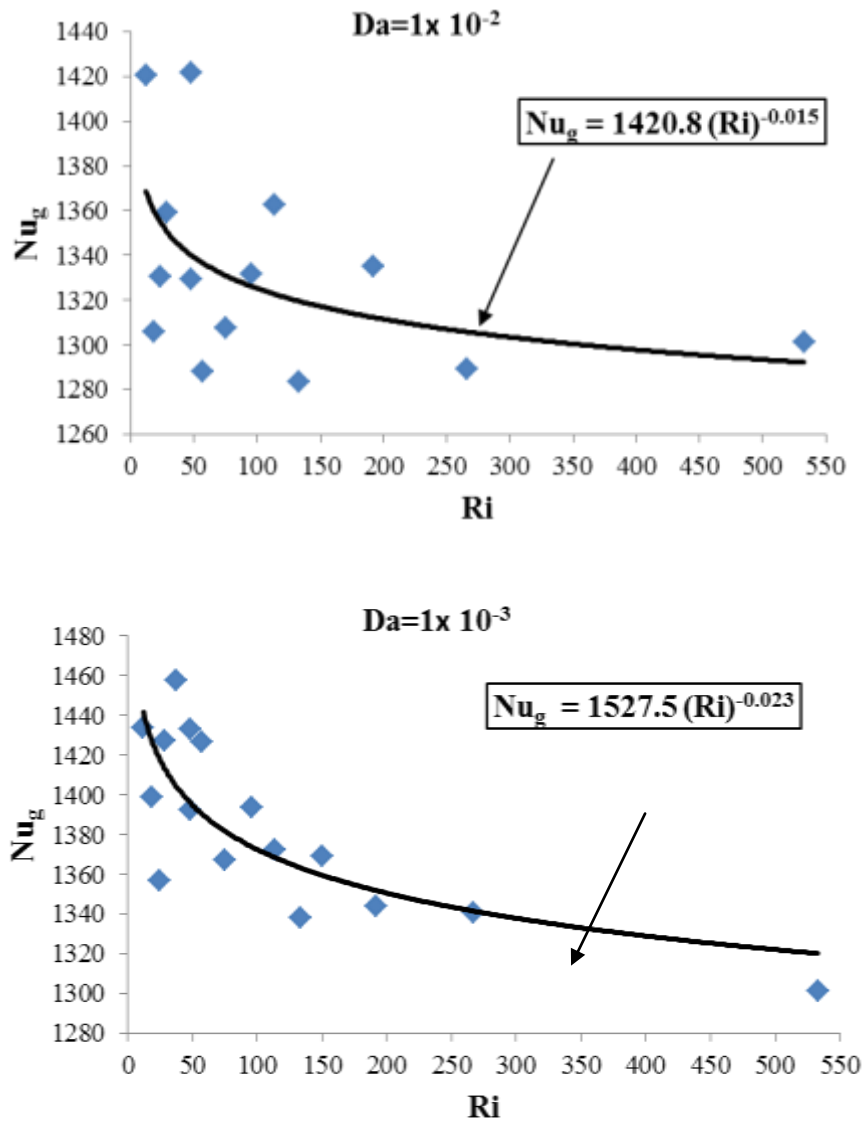


Figure 17. Global Nusselt number versus Richardson number.

REFERENCES

Ashby M.F., Evans A.G., Fleck, N.A., Gibson, L.J., Hutchinson, J.W. and Wadley, H.N.G., "Metal Foams: a Design Guide", Butterworth-Heinemann, Boston, MA, (2000).

Buonomo B., Manca O., Marinelli L., and Nardini S., "Mixed convection in horizontal channels heated below with external heat losses on upper plate and partially filled with aluminum foam", in "5th International Conference on Porous Media and Their Applications in Science, Engineering and Industry, Eds, ECI Symposium Series, Volume, (2014) .

Calmidi, V.V., and Mahajan, R.L. , "The effective Thermal Conductivity of High Porosity Metal Foams", ASME J. Heat Transfer ,121 ,pp. 466–471,(1999).

Chen C.C., Huang P.C., Hwang H.Y., "Enhanced forced convective cooling of heat sources by metal-foam porous layers", Int. J. of Heat and Mass Transfer,58:356–373, (2013)

Chikh S, Boumedien A, Bouhadek K, Lauriat G., " Analysis of Fluid Flow and Heat Transfer in Channel with Intermittent Heated Porous Blocks", Heat Mass Transfer, Vol. 33, pp.405–413,(1998) .

Fu WS, Huang HC, Liou WY., "Thermal Enhancement in Laminar Channel Flow with a Porous Block", Int J Heat Mass Transfer, Vol.39 ,pp.2165–2175,(1996) .

Guerroudj N. and Kahalerras H., "Mixed convection in a Channel Provided with Heated Porous Blocks of Various Shapes", Energy Conversion and Management, Vol. 51, pp. 505-517,(2010).

Hadim A., "Forced Convection in a Porous Channel with Localized Heat Sources", J Heat Transfer, Vol. 116, pp.465–471,(1994).

Holman J., P., "Heat Transfer", 10th Edition, McGraw-Hill Higher Education,(2010).

Huang P. C., and Vafai, K., "Analysis of Forced Convection Enhancements in a Channel Using Porous Blocks", Journal of Thermophysics and Heat Transfer, Vol. 8, No. 3, pp. 563-573,(1994).

Kurtbas I. and Celik N., "Experimental Investigation of Forced and Mixed Convection Heat Transfer in a Foam-Filled Horizontal Rectangular Channel", Int. J. Heat Mass Transfer , Vol. 52 , pp.1313–1325,(2009).

Nield D. A., and Bejan A., "Convection in Porous Media", New York, Springer,(2006).

Patankar S. V., "Numerical Heat Transfer and Fluid Flow", New York: Hemisphere,(1980).

Rachedi R. and Chikh S., "Enhancement of Electronic Cooling by Insertion of Foam Materials", Heat Mass Transf, Vol. 37, pp.371–378,(2001).

Vafai K, and Tien CL., "Boundary and Inertia Effects on Flow and Heat Transfer in Porous Media", Int J Heat Mass Transfer, Vol. 24, pp.193–203,(1981) .